Implementing MCMC: Multivariate estimation with confidence

James M. Flegal
Department of Statistics
University of California, Riverside
jflegal@ucr.edu

Rebecca P. Kurtz-Garcia
Department of Mathematical Science and Department of Statistical & Data Sciences
Smith College
rkurtzgarcia@smith.edu

August 29, 2024

Abstract

This paper addresses the key challenge of estimating the asymptotic covariance associated with the Markov chain central limit theorem, which is essential for visualizing and terminating Markov Chain Monte Carlo (MCMC) simulations. We focus on summarizing batching, spectral, and initial sequence covariance estimation techniques. We emphasize practical recommendations for modern MCMC simulations, where positive correlation is common and leads to negatively biased covariance estimates. Our discussion is centered on computationally efficient methods that remain viable even when the number of iterations is large, offering insights into improving the reliability and accuracy of MCMC output in such scenarios.

Keywords. Batch means, covariance matrix estimation, initial sequence estimators, Markov chain Monte Carlo, spectral variance.

1 Introduction

Since the groundbreaking publication by Gelfand and Smith (1990) Markov Chain Monte Carlo (MCMC) has played a crucial role in the utilization of Bayesian and frequentist statistical models. Usually, an MCMC algorithm generates a sequence of correlated observations to estimate multiple unknown quantities with respect to a target distribution,

which could include expectations, density functions, quantiles, modes, and more. Subsequently, the estimated quantities can be employed for inferential purposes. The main issues we address visualizing and terminating an MCMC simulation; and summarizing batching, spectral, and initial sequence covariance estimation techniques. Our emphasis is on providing recommendations for modern practical MCMC simulations where positive correlation is routine causing the estimated covariance to be negatively biased. Moreover, we focus on computationally viable techniques that are appropriate when the number of iterations is substantial.

Let F be a target probability distribution with support $\mathsf{X} \in \mathbb{R}^d$, $d \geq 1$. A common goal of an MCMC simulation is estimation of several unknown features of F. For example, suppose $g : \mathsf{X} \to \mathbb{R}^p$ be an F-integrable function and we are interested in estimating

$$\theta = E_F g(X) = \int_\mathsf{X} g(x) F(dx).$$

The p-dimensional vector θ could include moments, probabilities, or other features of F. For simplicity, we focus on features that can be expressed as expectations but will provide some discussions outside this setting where appropriate (such as quantiles).

Let $X = \{X_t, t \geq 1\}$ be a Harris ergodic Markov chain with invariant distribution F. We defer to other chapters in this volume as to how to produce such a Markov chain (see also Robert and Casella, 2004). Moreover, we assume a reasonable starting value, or starting distribution, has been identified (see e.g. Geyer, 2011; Vats et al., 2020). Then the ergodic theorem ensures we can estimate θ from a Monte Carlo sample of size n with the sample mean. That is, if $Y_i = g(X_i)$ for $i \geq 1$,

$$\bar{\theta}_n = \frac{1}{n} \sum_{i=1}^n Y_i \stackrel{a.s.}{\to} \theta \text{ as } n \to \infty. \tag{1}$$

Note that if (1) holds for any initial distribution then it holds for every initial distribution (Meyn and Tweedie, 2009).

Naturally there exists an unknown estimation error, $\bar{\theta}_n - \theta$, referred to as the Monte Carlo error. An approximate sampling distribution for the Monte Carlo error can be obtained via a Markov chain central limit theorem (CLT). An interested reader is directed to Jones (2004) for sufficient conditions for a Markov chain CLT and Jones and Hobert (2001) for an introduction on how to establish these conditions. We assume throughout such a CLT holds. That is, we assume there exists a $p \times p$ positive definite symmetric matrix Σ such that

$$\sqrt{n} \left(\bar{\theta}_n - \theta \right) \stackrel{d}{\to} \mathrm{N}_p \left(0, \Sigma \right) \text{ as } n \to \infty, \tag{2}$$

where

$$\Sigma = \sum_{k=-\infty}^{\infty} R(k) \tag{3}$$

and $R(k) = \text{Cov}_F [Y_1, Y_{1+k}]$ is the lag-k covariance matrix. Similar to the ergodic theorem, if (2) holds for any initial distribution then it holds for every initial distribution (Meyn and Tweedie, 2009).

The matrix Σ is referred to as the asymptotic covariance associate with a Markov chain CLT, or more simply as the long run variance (LRV). Since Σ is positive definite there is exactly one positive definite matrix B such that $\Sigma = B^T B$, where B is the positive square root. Moreover, Monte Carlo standard errors (MCSEs) for each component of θ can be obtained by estimating the vector of length p given by $\text{diag}(B)/\sqrt{n}$. Hence, one can use the CLT at (2) to access variability of the estimator $\bar{\theta}_n$ provided an estimate of Σ, say Σ_n, is available. We explore three broad classes of estimators appropriate for this task.

The rest of the chapter is organized as follows. Section 2 describes a number of multivariate MCMC output analysis tools based on (2) that require high-quality estimates of Σ. Section 3 considers batching estimators for Σ and introduces the lugsail transformation. Section 4 summarizes spectral variance (SV) estimators for Σ and the role lag windows play in their construction. Section 5 introduces initial sequence estimators for Σ, which leverage the properties of the sequence of lag-k covariance matrices leading to conservative estimates. Section 6 illustrates these variance estimation techniques using a Bayesian logistic regression for modeling credit risk that specifically compares finite sample performance and computational time. We conclude with a discussion in Section 7.

2 MCMC output analysis

A crucial step in a MCMC experiment is considering the Monte Carlo error resulting from finite simulation. In short, it's advisable to include individual MCSEs or marginal confidence intervals to assess the variability of the estimator(s) $\bar{\theta}_n$, as emphasized by Flegal et al. (2008). Additionally, practitioners can use the Monte Carlo error to help determine the simulation's duration.

Practitioners can address these aspects in conjunction by employing a sequential stopping rule that terminates the simulation when the confidence interval width for the estimator(s) of interest reaches a user-defined threshold, as discussed by Jones et al. (2006). Alternatively, an extension of this rule can be used which terminates the simulation when computational uncertainty becomes sufficiently small compared to posterior uncertainty. Specifically, Flegal and Gong (2015) propose a relative sequential stopping rule that ter-

minates when the confidence interval width is sufficiently small relative to the posterior standard deviation of the target parameter. Gong and Flegal (2016) establish that this approach is equivalent to stopping when the effective sample size (ESS) is adequately large.

Both methods critically rely on estimates for the diagonal entries of Σ, which are used to estimate of $\text{diag}(B)/\sqrt{n}$. Recent advancements in MCMC output analysis incorporate correlation information from the off-diagonal elements of Σ. We next provide an overview of such an approach and relevant features, underlining the necessity for accurate multivariate estimation techniques of Σ.

2.1 Multivariate sequential stopping rule

For simplicity, consider the p-dimensional vector of sample means $\bar{\theta}_n$ in (1). Suppose $\chi^2_{1-\alpha,p}$ denotes a $1-\alpha$ quantile from a χ^2 distribution with p degrees of freedom and $|\cdot|$ is the determinant. Then an asymptotic $100(1-\alpha)\%$ confidence region can be constructed as

$$C_\alpha(n) = \left\{ n(\bar{\theta}_n - \theta)^T \Sigma_n^{-1} (\bar{\theta}_n - \theta) < \chi^2_{1-\alpha,p} \right\}.$$

The p-dimensional ellipsoid $C_\alpha(n)$ has volume

$$\text{Vol}\left(C_\alpha(n)\right) = \frac{2\pi^{p/2}}{p\Gamma(p/2)} \left(\frac{\chi^2_{1-\alpha,p}}{n} \right)^{p/2} |\Sigma_n|^{1/2} \ ,$$

which can be used to measure the variability of the estimator $\bar{\theta}_n$.

Practitioners can terminate the simulation when the computational uncertainty is small relative to the model uncertainty in multivariate settings. To this end, suppose the model uncertainty is measured using the generalized variance of the target F, i.e. $|\Lambda|$ where $\Lambda = \text{Var}_F(Y_1)$. We can estimate Λ with the sample covariance matrix, denoted as Λ_n. A relative standard deviation sequential fixed-volume stopping rule, proposed by Vats et al. (2019), terminates the simulation when the ellipsoid volume is sufficiently small relative to the volume of Λ_n. That is, the simulation terminates when the volume of $C_\alpha(n)$ is an ϵ^{ith} fraction of the size of Λ_n for some desired tolerance level $\epsilon > 0$. Formally, the fixed-volume stopping rule terminates the first time

$$\left\{ \text{Vol}\left(C_\alpha(n)\right)^{1/p} + 1/n < \epsilon |\Lambda_n|^{1/2p} \right\}, \tag{4}$$

for $n > n^* > 0$. The role of n^* is to ensure stable estimates for Λ and Σ have been obtained. While there is no theoretical restrictions on n^*, we elaborate on a reasonable choice later.

The fixed-volume stopping rule is asymptotically equivalent to simulating until a (mul-

tivariate) ESS is sufficiently large. Specifically, ESS measures the sample size required to achieve the same generalized Monte Carlo error if the sample was from an independent and identically distributed sequence, defined as

$$\text{ESS} = n \left(\frac{|\Lambda|}{|\Sigma|} \right)^{1/p}.$$

Since ESS is unknown, it is estimated using

$$\widehat{\text{ESS}} = n \left(\frac{|\Lambda_n|}{|\Sigma_n|} \right)^{1/p}. \tag{5}$$

When $p = 1$, (5) reduces to the typical estimate of univariate ESS (Kass et al., 1998; Robert and Casella, 2004). Since the ratio of generalized variances in (5) also appears in (4), the fixed-volume stopping rule can be shown to be asymptotically equivalent terminating when

$$\widehat{\text{ESS}} \geq M_{\alpha,\epsilon,p},$$

where $M_{\alpha,\epsilon,p}$ depends only on the confidence level, relative precision desired, and dimension of the estimation problem. Hence $M_{\alpha,\epsilon,p}$ can be calculated prior to simulation, which is available via the `minESS` function (Flegal et al., 2021). For example, suppose we are interested terminating the simulation when the volume of a 95% confidence region ($\alpha = 0.05$) is 0.05 the volume of a posterior covariance matrix Λ. Then dimensions p of 1, 3, or 10 would yield $M_{\alpha,\epsilon,p}$ of 6146, 8123, or 8831, respectively. The value $M_{\alpha,\epsilon,p}$ provides a reasonable choice for a minimum simulation size n^*.

Vats and Knudson (2021) establish a relationship between ESS and the Gelman-Rubin-Brooks diagnostic (Brooks and Gelman, 1998; Gelman and Rubin, 1992), which is also used as a stopping criteria. However, we recommend using fixed-volume or ESS stopping rules since they are easily interpretable, have lower variability, and are readily available in software.

Example 1. Consider the three-component normal mixture density

$$f(x) = .2\phi(x; 2.5, 1^2) + .3\phi(x; 4.5, 1^2) + .5\phi(x; 7.5, 1^2), \tag{6}$$

where $\phi(x; m, s^2)$ denotes a normal density function with mean m and variance s^2. We simulate $5e4$ correlated samples from this density via a random walk Metropolis-Hasting algorithm with proposal standard deviation of $1/2$.

The left panel of Figure 1 plots the correlation coefficient against the lag where the observed lag 1 autocorrelation is approximately 0.98. While this high level of correlation

suggest a larger proposal variance should be considered, we continue using this Metropolis-Hastings update for illustrative purposes. Consider estimating $E_F X$, which we know to be 5.6 from (6), using $\bar{x} = 5.5493$ with an MCSE of 0.11549. The ESS based on estimation of the mean can also be estimated as $\widehat{\text{ESS}} = 386$. Since this is lower than $M_{.05,.10,1} = 1536$, it appears the simulation should continue to ensure higher accuracy in estimation of the mean.

2.2 Visualizing simultaneous simulation error

Up to this point we have only considered expectations, however estimation of quantiles associated with F are often of interest. For example when F is a posterior, the quantile of interest could be from a marginal posterior distribution. Let $h : \mathcal{X} \to \mathbb{R}$ and $V = h(X)$ with distribution function $F_h(v)$. Further assume $F_h(v)$ is absolutely continuous with a continuous density $f_h(v)$. Then define the q-quantile associated with F_h as

$$\xi_q = F_h^{-1}(q) = \inf\{v : F_h(v) \geq q\}.$$

The quantile ξ_q can be estimated using $\hat{\xi}_q = h(X)_{\lceil nq \rceil : n}$, which is the $\lceil nq \rceil^{th}$ order statistic of $h(X)$. Doss et al. (2014) establish conditions under which the sampling distribution of the Monte Carlo error is approximately normal and provide techniques to estimate the associated LRV.

Estimation on a finite combination of p expectations and quantiles can also lead to a joint sampling distribution. An interested reader is directed to Robertson et al. (2021) for conditions that ensure such a CLT holds and practical techniques to estimate the associated $p \times p$ positive definite LRV Ω. In short, define the p-vector ν containing the expectations and quantiles that we aim to estimate with the p-vector $\hat{\nu}$ the corresponding ergodic averages and order statistics, then as as $n \to \infty$, we assume

$$\sqrt{n}\,(\hat{\nu} - \nu) \xrightarrow{d} N_p\,(0, \Omega)\,. \tag{7}$$

After simulating n MCMC iterations, practitioners may want to visualize the results of MCMC experiments and corresponding variability. However, visualizing a p-dimensional ellipsoid is difficult beyond two dimensions and plots of multiple marginal intervals can be difficult to interpret. To this end, Robertson et al. (2021) also provide p-dimensional simultaneous confidence regions for ν using (7) and a strongly consistent estimator of Ω,
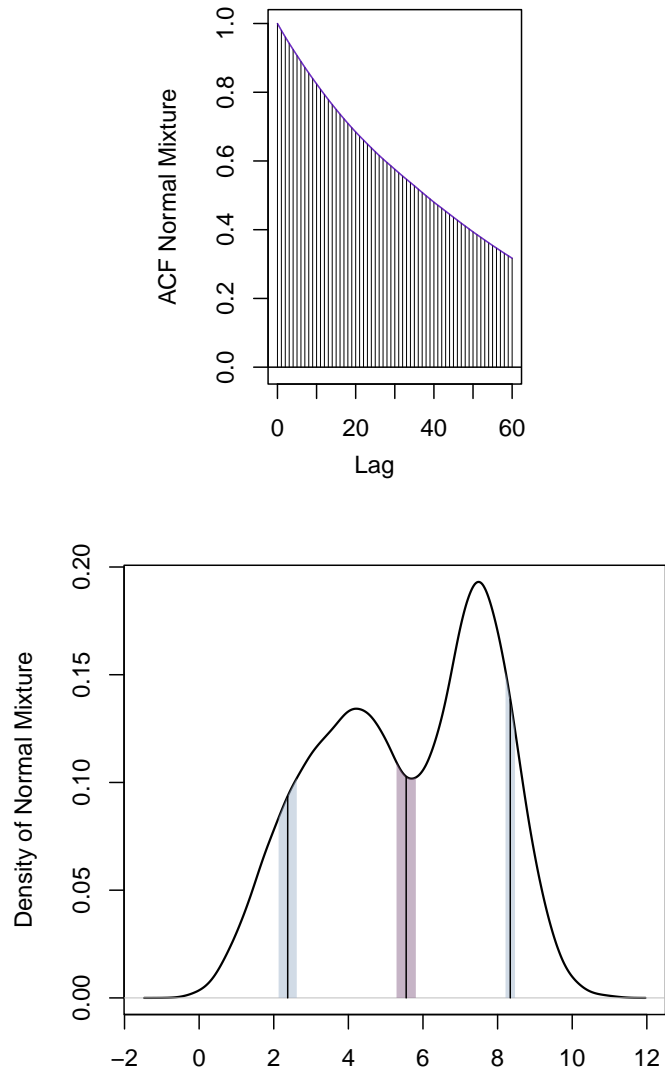
Figure 1: Normal mixture density ACF plot and nonparametric density plot with simultaneous error bars surrounding estimates of the mean and endpoints of an 80% credible interval.

say $\hat{\Omega}$. Their approach considers hyperrectangular regions of the form

$$C_{SI}(z) = \prod_{i=1}^{p} \left[\hat{\nu}_i - z\frac{\hat{\Omega}_{i,i}}{n}, \hat{\nu}_i + z\frac{\hat{\Omega}_{i,i}}{n} \right],$$ (8)

where $z > 0$.

Then they propose a parametric approach to find z^* such that $C_{SI}(z^*)$ has a user-defined simultaneous coverage probability $1 - \alpha$. Specifically, suppose $U \sim N_p(\hat{\nu}, \hat{\Omega}/n)$ and notice that $\Pr(U \in \mathcal{C}_{SI}(z))$ is strictly increasing as $z > 0$ increases. Then a univariate optimization can be implemented to find z^* such that $\Pr(U \in \mathcal{C}_{SI}(z^*)) \approx (1 - \alpha)$ where the multivariate normal probabilities can be quickly and accurately calculated using quasi-Monte Carlo methods (Genz et al., 2018). Finally, the marginal intervals at (8) can be incorporated into standard plots enabling practitioners to more easily assess the reliability of an MCMC simulation through visual tools. The following example illustrates one such visualization of the simultaneous simulation error.

Example 2. Recall the three-component normal mixture density at (6) where $5e4$ correlated samples were obtained from a random walk Metropolis-Hasting algorithm. We now consider simultaneous estimation of the mean $E_F X$ and an 80% credible interval for X with endpoints $\xi_{.10}$ and $\xi_{.90}$, where under regularity conditions as $n \to \infty$,

$$\sqrt{n}\left(\begin{pmatrix} \bar{x}_n \\ \hat{\xi}_{.10} \\ \hat{\xi}_{.90} \end{pmatrix} - \begin{pmatrix} E_F X \\ \xi_{.10} \\ \xi_{.90} \end{pmatrix} \right) \xrightarrow{d} N_3\left(0, \Omega\right).$$

The right panel of Figure 1 plots the estimated mean and 80% credible interval along with a nonparametric density estimate of $f(x)$. The error bars around the mean and quantiles account for the correlated nature of the process and have a simultaneous nominal 0.95 coverage probability.

The accuracy of inference and estimated ESS in the preceding example are significantly affected by the LRV estimation quality. If the LRV is underestimated, it can lead to smaller than appropriate MCSEs, which in turn results in an inflated ESS and excessively narrow simultaneous (or univariate) error bars. The following sections introduce three distinct techniques for estimating Σ. These techniques are particularly valuable in scenarios with large sample sizes and high correlations, which are common in MCMC simulations.

3   Batching methods

In MCMC simulations the batch means (BM) estimator for Σ is most commonly implemented since it's easy to use and computationally efficient (Chen and Seila, 1987; Geyer, 1992). The BM estimator uses a sequential non-overlapping batches of length b to estimate Σ. Suppose $n = ab$ and let $\bar{Y}_k = b^{-1} \sum_{i=1}^{b} Y_{kb+i}$ for $k = 0, \ldots, a-1$. Then the BM estimator with batch size b is,

$$\hat{\Sigma}_{n,b} = \frac{b}{a-1} \sum_{k=0}^{a-1} \left(\bar{Y}_k - \bar{\theta}_n \right) \left(\bar{Y}_k - \bar{\theta}_n \right)^T . \tag{9}$$

The BM estimator has been well studied in MCMC settings (Chakraborty et al., 2022; Flegal and Jones, 2010; Jones et al., 2006; Vats et al., 2019). However, BM estimators suffer from negative bias in finite samples when the Markov chain has positive correlation. A careful discussion of the bias requires defining

$$\Gamma = - \sum_{k=-\infty}^{\infty} k R(k) .$$

Then the bias of the BM estimator can be obtained, i.e.

$$\text{Bias}\left(\hat{\Sigma}_{n,b}\right) = \frac{\Gamma}{b} + o\left(\frac{1}{b}\right) .$$

The first-order bias term, Γ/b, has negative diagonals for positively correlated processes. Moreover the magnitude of the negative bias grows as the correlation approaches 1.

To address this bias, Vats and Flegal (2022) propose a linear combination of two BM estimators with batch sizes b and $\lfloor b/r \rfloor$ for $r \geq 1$. Specifically, if $c_n \in [0,1)$ then the lugsail BM estimator is

$$\hat{\Sigma}_{n,L} = \frac{1}{1-c_n} \hat{\Sigma}_{n,b} - \frac{c_n}{1-c_n} \hat{\Sigma}_{n,\lfloor b/r \rfloor} . \tag{10}$$

When $r = 1/c_n$ the estimator (10) has a first-order bias of 0, which has been referred to as the zero lugsail BM estimator or flat-top BM estimator (Liu and Flegal, 2018). More generally, Vats and Flegal (2022) show

$$\text{Bias}\left(\hat{\Sigma}_{n,L}\right) = \frac{\Gamma}{b}\left(\frac{1-rc_n}{1-c_n}\right) + o\left(\frac{1}{b}\right) . \tag{11}$$

Hence, setting $r > 1/c_n$ can induce a positive first-order bias for positively correlated chains.

Vats and Flegal (2022) provide recommendations for r and c_n based on estimating the underlying lag 1 autocorrelation of the Markov chain. When the underlying correlation is low, $\rho \in [0, .7)$, the authors suggest setting $r = 2$ and $c_n = 1/2$ resulting in a zero lugsail

BM estimator. For moderate correlation settings, $\rho \in [.7, .95)$, they suggest an adaptive lugsail where $r = 2$ and c_n varies based on n but ultimately converges to the zero lugsail BM estimator. Specifically,

$$c_n = \frac{\log(n) - \log(b) + 1}{2(\log(n) - \log(b)) + 1} .$$

For high correlation settings, $\rho \in [.95, 1)$, they suggest setting $r = 3$ and $c_n = 1/2$ resulting in an over lugsail BM estimator. The first-order bias for the over lugsail setting is intentionally over corrected to account for higher-order and finite sampling biases that also lead to underestimating Σ in practice. Since the over lugsail tends to overestimate Σ while remaining asymptotically unbiased, it is particularly useful in conjunction with sequential stopping rules. A downside of lugsail estimators is that they have a higher variance than the standard BM estimator for fixed b.

The following example illustrates the utility of lugsail estimators with a univariate data set. Calculations in the example utilize the exact bias expression of Aktaran-Kalaycı et al. (2007) for the univariate BM estimator, i.e. when $p = 1$

$$\text{Bias}\left(\hat{\Sigma}_{n,b}\right) = -\frac{2(a+1)}{ab} \sum_{s=1}^{b-1} sR(s) - 2 \sum_{s=b}^{\infty} R(s) - \frac{2}{a-1} \sum_{s=b}^{n-1} \left(1 - \frac{s}{n}\right) R(s) .$$

This result enables exact bias calculations for lugsail estimators due to the linear relationship at (10).

Example 3. The normal AR(1) times series is given by

$$X_{n+1} = \phi X_n + \epsilon_n ,$$

where the ϵ_n are i.i.d. $N(0,1)$ and $|\phi| < 1$. This Markov chain has invariant distribution $N\left(0, 1/(1 - \phi^2)\right)$. When estimating the mean of this distribution, $E_F X = 0$, $\Sigma = 1/(1-\phi)^2$ and $\text{ESS}/n = (1 - \phi)^2/(1 - \phi^2)$. We investigate two scenarios with correlation coefficients, denoted as moderate ($\phi = 0.92$) and high ($\phi = 0.98$), respectively. Our aim is to demonstrate the impact of bias on coverage probability and ESS calculations in finite sample contexts. For simplicity $b = \lfloor \sqrt{n} \rfloor$ in this example.

In Figure 2, the observed coverage probability of a 95% confidence interval for $E_F X$, using various variance estimation methods, is depicted. The original BM estimator gradually approaches the nominal level of 0.95, suggesting an underestimation of finite sample confidence intervals. This underestimation is notably in both scenarios, where the coverage probability hovers around 0.935 after $2e5$ iterations when $\phi = 0.92$. Although this deviation might seem minor, it becomes magnified in multivariate applications like the simultaneous
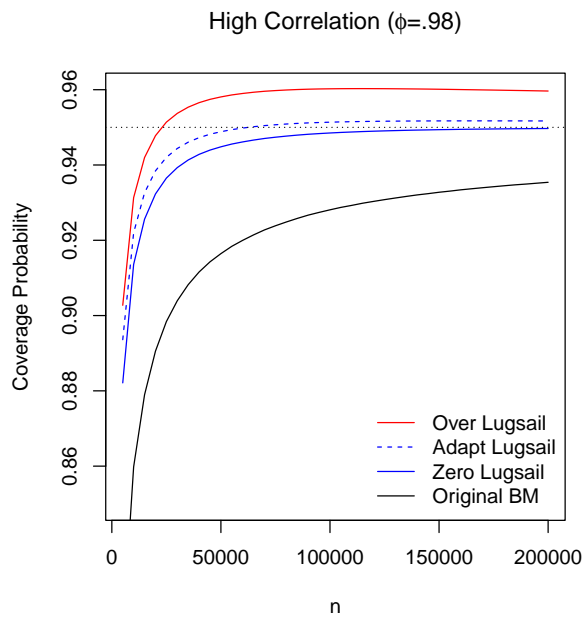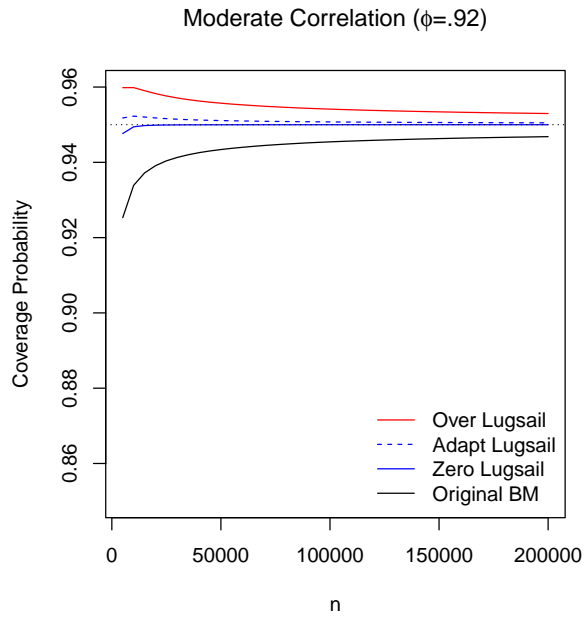
10

Figure 2: Coverage probability of a 95% confidence interval for $E_F X$, using various variance estimation methods.

confidence regions demonstrated in Figure 1.

Both the zero and adapt lugsail estimators similarly tend to converge towards the expected value from below, albeit at a faster rate. The advantage of the over lugsail estimator lies in its behavior of converging from above in both correlation settings, following an initial simulation effort. This has a statistical advantage in that the observed coverage probability will at least obtain the nominal confidence level of 95%, satisfying the requirements for a valid Neyman-Pearson inference procedure.

Consistent findings are drawn from Figure 3, where the relationship between simulation size and expected ESS/n is depicted for different variance estimation techniques. The dotted horizontal black line corresponds to the actual ESS/n, which varies with ϕ. The advantage of converging from below exhibited by the over lugsail estimator is that it guards against premature termination of simulations. Subsequent examples, where the true value cannot be calculated, will exhibit similar patterns.

Choosing the batch size b is critical to the finite sample behaviour of the BM estimator. The lugsail BM estimator requires that both the number of batches $a \to \infty$ and batch size $b \to \infty$ as $n \to \infty$ to obtain strong and mean-square consistency. For the BM estimator, Flegal and Jones (2010) establish the mean-squared-optimal batch size $b \propto n^{1/3}$, where as Liu et al. (2021) provides a parametric approach to estimate the proportionality constant. This proportionality constant is a function of Σ and Γ and hence depends on the amount of serial correlation in the Markov chain.

Batch size selection for the more general lugsail BM estimator remains an open problem. For example, an optimal batch size for the zero lugsail estimator should be smaller than that of the standard BM estimator. However, a mean-squared-optimal approach based solely on the first order bias would net an optimal b value that minimizes only the variance by setting $b = 0$. Hence a more nuanced approach is necessary. Fortunately, current best practices are readily available to practitioners in the `mcmcse` R package (Flegal et al., 2021).

3.1 Other batch based estimators

There are a number of additional batch based estimators of Σ. Overlapping BM use $n-b+1$ overlapping batches of length b denoted $\dot{Y}_l(b) = b^{-1} \sum_{t=1}^{b} Y_{l+t}$ for $l = 0, \ldots, n - b$. Then the overlapping BM estimator is given by

$$\hat{\Sigma}_{obm} = \frac{nb}{(n-b)(n-b+1)} \sum_{l=0}^{n-b} (\dot{Y}_l(b) - \bar{Y}_n)(\dot{Y}_l(b) - \bar{Y}_n)^T. \tag{12}$$
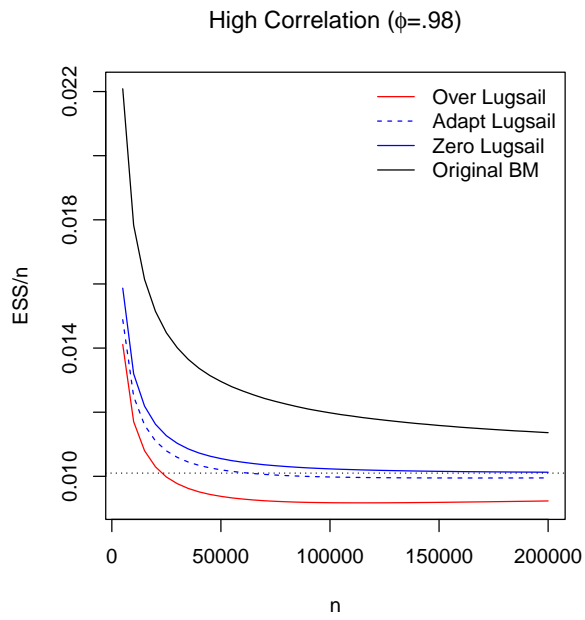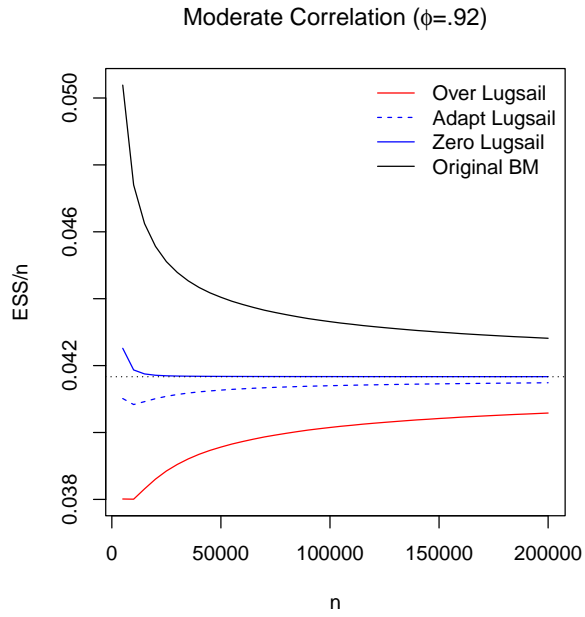
Figure 3: Plots of simulation size versus ESS/n, using various variance estimation methods.

The first-order bias of overlapping BM is equivalent to that of the BM estimator but computing overlapping BM is slower given the increased quantity of batches. One advantage of overlapping BM is a reduction in its variability. Specifically, the variance of the BM estimator is 1.5 times higher than that of the overlapping BM estimator (Flegal and Jones, 2010).

One could consider a linear combination of overlapping BM estimators, similar to (10). This remains an open problem but the first-order bias will remain equal to (11). Other BM variants include a recursive estimator which employs a sequence of batch sizes that increase as n increases (Chan and Yau, 2017) and a replicated estimator for estimating Σ from parallel Markov chains (Argon and Andradóttir, 2006; Gupta and Vats, 2020).

Lag windows, introduced the following section, can also be incorporated in to batched estimators. To this end, Damerdji (1987, 1991) and Vats et al. (2018) study a generalized overlapping BM estimator and establish that it is asymptotically equivalent to SV estimators. Liu and Flegal (2018) consider a multivariate non-overlapping version, which they refer to as weighted BM. Use of these with the Bartlett lag window leads to the BM and overlapping BM estimators at (9) and (12). Using the Bartlett flat-top lag window in the weighted BM estimator leads the the zero lugsail BM estimator.

4   Spectral methods

SV methods can also be used to estimate Σ in MCMC simulations (Flegal and Jones, 2010; Vats et al., 2018). First consider estimating the lag-k covariance matrix $R(k)$ with the sample lag-k covariance

$$\hat{R}(k) = \frac{1}{n} \sum_{i=1}^{n-k} \left(Y_i - \bar{\theta}_n \right) \left(Y_{i+s} - \bar{\theta}_n \right)^T . \tag{13}$$

SV estimators weight the sample lag covariances in (13) using a lag window function $\kappa :$ $\mathbb{R} \to \mathbb{R}$ such that $\kappa(0) = 1, \kappa(x) = \kappa(-x)$ for all $x \in \mathbb{R}$. Suppose $b \in \mathbb{N}$ is the truncation point, then the multivariate SV estimator is

$$\dot{\Sigma}_{k,b} = \sum_{s=-(n-1)}^{n-1} \kappa\left(\frac{s}{b}\right) \hat{R}(s) . \tag{14}$$

Table 1 provides some common lag windows, which are also plotted in Figure 4. The Bartlett lag-window is the most popular and routinely referred to as the Newey and West (1987) estimator in econometrics. It is well known the overlapping BM estimator at (12) is

Table 1: Common lag windows.

Lag Window	$\kappa(x) =$
Bartlett	$(1 - |x|)\, I(|x| \leq 1)$
Bartlett Flat-Top	$I\left(|x| \leq \dfrac{1}{2}\right) + 2\left(1 - |x|\right) I\left(\dfrac{1}{2} < |x| \leq 1\right)$
Tukey-Hanning	$\dfrac{1}{2} + \dfrac{1}{2}\cos(\pi x) I(|x| \leq 1)$
Quadratic Spectral	$\dfrac{25}{12\pi^2 x^2}\left\{\dfrac{\sin\left(6\pi x/5\right)}{6\pi x/5} - \cos\left(6\pi x/5\right)\right\}$

asymptotically equal to the SV estimator with a Bartlett lag window apart from some end effects (see e.g. Meketon and Schmeiser, 1984; Vats et al., 2019; Welch, 1987).

Figure 4 illustrates Bartlett, Tukey-Hanning, and Quadratic Spectral lag windows decrease for $x \in [0, \epsilon)$ for some $\epsilon > 0$, which leads to underestimation of Σ for positively correlated sequences. The Bartlett flat-top lag window (Politis and Romano, 1995, 1996) has a slope of zero at $x = 0$ and as a result has a first-order bias of zero.

The general first-order bias expression depends on the smoothness of the kernel at zero, and requires more notation. To this end, define

$$k_q = \lim_{x \to 0} \frac{1 - k(x)}{|x|^q}$$

for $q \in [0, \infty)$. If we let $q \geq 1$ be the largest integer for which $k_q < \infty$ we will observe that smoother kernels near 0 result larger values of q, see Andrews (1991) and Parzen (1957) for additional discussion. A key object in a general first-order bias expression is

$$\Gamma^{(q)} = -\sum_{k=-\infty}^{\infty} k^q R(k)\,,$$

which generalizes Γ. Then the bias of the SV estimator can be obtained, i.e.

$$\text{Bias}\left(\dot{\Sigma}_{k,b}\right) = \frac{k_q \Gamma^{(q)}}{b^q} + o\left(\frac{1}{b^q}\right)\,.$$

Again, the first-order bias term, $k_q \Gamma^{(q)}/b^q$, has negative diagonals for positively correlated processes and the magnitude of the negative bias grows as the correlation approaches 1.

Lugsail lag windows of Vats and Flegal (2022) generalize traditional lag windows and
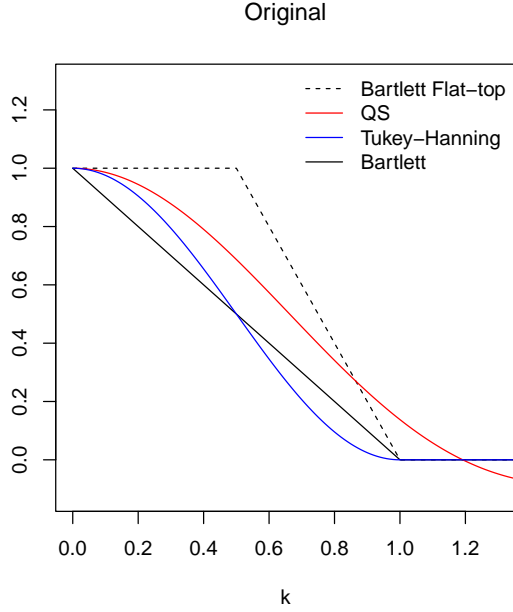
Figure 4: Plots of original lag windows.

allow settings that lift the weights above 1 to induce a positive first-order bias. Suppose $r \geq 1$ and $c_n \in [0,1)$ is a sequence such that $c_n \to c$ as $n \to \infty$, then the family of lugsail windows associated any existing lag window κ is defined as

$$\kappa_L(x) = \frac{1}{1 - c_n}\kappa(x) - \frac{c_n}{1 - c_n}\kappa(rx).$$

(15)

Setting $c_n = 0$ or $r = 1$ results in the original lag window. Using the Bartlett lag window with $r = 2$ and $c_n = 2$ gives the Bartlett flat-top lag window in Table 1. The left panel of Figure 5 shows zero lugsail versions of the Bartlett, Tukey-Hanning, and Quadratic Spectral lag windows, which have a first-order bias of zero. The right panel of Figure 5 shows over lugsail versions of the same three lag windows, which have a positive first-order bias in a effort to offset most of the (unknown) high-order bias terms.

The lugsail lag window with the multivariate SV estimator can alternatively be characterized as a linear combination of SV estimators with truncation points b and $\lfloor b/r \rfloor$. That is, the lugsail SV estimator is

$$\dot{\Sigma}_{k,L} = \frac{1}{1 - c_n}\dot{\Sigma}_{k,b} - \frac{c_n}{1 - c_n}\dot{\Sigma}_{k,b/r}.$$

(16)

From this linear relationship we observe that the lugsail estimators retain weak and strong
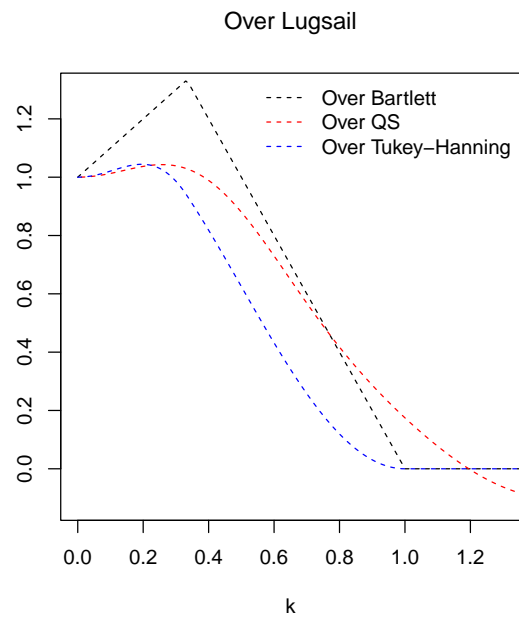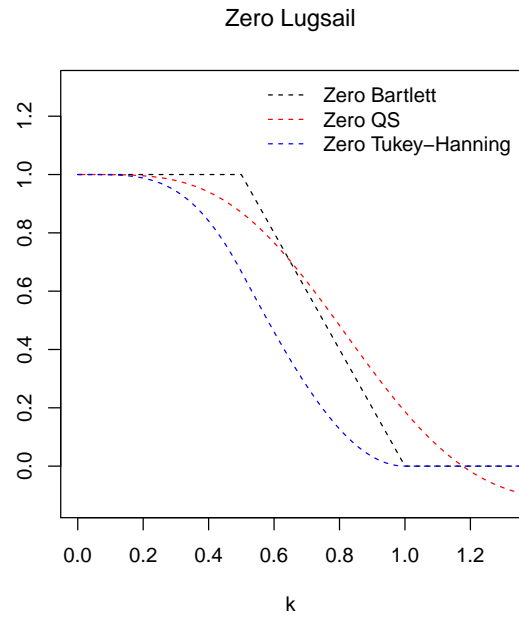
16

Figure 5: Plots of zero and over lugsail versions of the Bartlett, Tukey-Hanning, and Quadratic Spectral lag windows.

consistency from the original SV estimators, sufficient conditions can be found in Vats et al. (2018). Vats and Flegal (2022) establish the first-order bias expression for lugsail lag windows

$$\text{Bias}\left(\dot{\Sigma}_{k,L}\right) = \frac{k_q \Gamma^{(q)}}{b^q} \left(\frac{1 - r^q c_n}{1 - c_n}\right) + o\left(\frac{1}{b^q}\right),$$

where, setting $r > 1/c_n$ can again induce a positive first-order bias for positively correlated chains.

Choosing the truncation point b crucially impacts the finite sample behaviour of the SV estimator. The literature on optimal truncation points, which is also referred to as automatic bandwidth procedures, is far richer for SV estimators compared to optimal batch sizes for BM estimators. An interested reader is directed to Andrews (1991), Chang et al. (2021), Lazarus et al. (2021), Lazarus et al. (2018), Sun (2013, 2014), and Sun and Phillips (2008).

SV estimators offer greater flexibility compared to batching methods, as they provide a range of lag windows to choose from (see e.g. Anderson, 1994). However, SV estimators are less commonly utilized in practical MCMC simulations due to their slower calculation speeds. A potential remedy involves leveraging the efficiency of a fast Fourier transform to level the computation times. This strategy has been implemented in the `mcmcse` R package (Flegal et al., 2021) and will be employed for comparing computational efficiency in Section 6.

5 Initial sequence estimators

Geyer (1992) introduced a conservative Monte Carlo error estimation method for a univariate mean, which was extended to multivariate settings by Kosorok (2000) and Dai and Jones (2017). The fundamental concept involves leveraging the properties of the sequence of lag-k covariance matrices to establish a truncation point for the truncated periodogram lag-window. A more intricate shape-constrained estimator for univariate scenarios is considered by Berg and Song (2022). This class of estimators is appropriate for reversible Markov chains, i.e. those that satisfy detailed balance with respect to F. Consequently, in this section we assume $R(k) = R(-k)$ for all integers k.

We confine our focus to multivariate initial sequence estimates of Σ from Dai and Jones (2017). To this end, define the sum of an adjacent pair of covariances by $A_i = R(2i) + R(2i + 1)$ for $i = 0, 1, 2, \ldots$. Then Σ can be rewritten as

$$\Sigma = -R(0) + 2 \sum_{i=0}^{\infty} A_i$$

and the mth partial sum can be defined as

$$\Sigma_m = -R(0) + 2\sum_{i=0}^{m} A_i.$$

Dai and Jones (2017) show there exists a non-negative integer m_0 such that Σ_m is positive definite for $m \geq m_0$ and not positive definite for $m < m_0$. They go on to prove the sequence $\{|\Sigma_m| : m_0, m_0 + 1, \dots\}$ is positive, increasing, and converges to $|\Sigma|$, which can be used to establish a truncation point in practice.

Recall the sample lag covariances at (13) and define $\hat{A}_i = \hat{R}(2i) + \hat{R}(2i+1)$ for $i = 0, 1, 2, \dots$. Then the empirical estimator of Σ_m for $0 \leq m \leq \lfloor n/2 - 1 \rfloor$ is

$$\Sigma_{n,m} = -\hat{R}(0) + 2\sum_{i=0}^{m} \hat{A}_i.$$

Let s_n be the smallest integer such that Σ_{n,s_n} is positive definite, which we know exists when n is sufficiently large. Further, let t_n be the largest integer $m \in \{s_n, \dots, \lfloor n/2 - 1 \rfloor\}$ where $|\Sigma_{n,i}| > |\Sigma_{n,i-1}|$ for all $i \in \{s_n + 1, \dots, m\}$. Then Dai and Jones (2017) define the multivariate initial sequence estimate as $\Sigma_{\mathrm{seq},n} = \Sigma_{n,t_n}$. The multivariate initial sequence estimate is conservative since $\liminf_{n\to\infty} |\Sigma_{\mathrm{seq},n}| \geq |\Sigma|$ with probability 1.

The estimator $\Sigma_{\mathrm{seq},n}$ is constructed sequentially using the update

$$\Sigma_{n,i+1} = \Sigma_{n,i} + 2\hat{A}_{i+1}.$$

Since $\hat{A}_{i+1}$ could potentially have negative eigenvalues, Dai and Jones (2017) suggest an adjusted update where negative eigenvalues are replaced by 0 at each step. This process yields the adjusted multivariate initial sequence estimator, say $\Sigma_{\mathrm{adj},n}$, which is also conservative in the sense that $\liminf_{n\to\infty} |\Sigma_{\mathrm{adj},n}| \geq |\Sigma|$ with probability 1.

Initial sequence estimators find limited use among MCMC practitioners due to their applicability only to reversible Markov chains. Moreover, bias and variance properties of initial sequence estimators remain unknown. Most critical to practitioners, initial sequence estimators also require greater computational effort. We elaborate on these restrictions in the following section where all the calculations are readily available through the `mcse.initseq()` function within the `mcmcse` R package.

6   Example

We highlight differences of the BM, SV, and initial sequence estimators of Σ using Bayesian logistic regression for modeling credit risk. The dataset utilized is sourced from UC Irvine's machine learning repository (Hofmann, 1994). The model we pursue aims to classify loan applicants into low and high credit risk groups using seven explanatory variables; status of existing checking account, credit history, duration, savings, other debts, housing status, and amount.

Given that some explanatory variables are categorical, the proposed model contains 19 regression coefficients, including the intercept term. The Bayesian logistic regression model is represented as

$$P(Y_i = 1) = \frac{\exp\left(x_i^T \beta\right)}{1 + \exp\left(x_i^T \beta\right)}.$$

We consider a multivariate normal prior distribution $\beta \sim N(0, \frac{1}{100}I_{19})$ and are interested in estimating posterior means for the 19 regression coefficients. We sample from the resulting posterior using a Metropolis-Hastings sampler via the `MCMCpack R` package.

Variability in the posterior mean estimates can be ascertained via estimation of an appropriate covariance matrix Σ, which can then be used to calculate MCSEs. Instead, we consider ESS as a proxy for the MCSE because ESS is univariate and the quality of estimation of both MCSE and ESS are largely dependent on the estimation of Σ. Specifically, we consider $\widehat{\text{ESS}}/n$ calculated using BM, SV, and initial sequence estimators of Σ with their corresponding the original, zero, and over lugsail settings (when appropriate). ESS was estimated using the `R` package `mcmcse` with BM, SV (with the Bartlett lag window), and initial sequence estimators. Chain lengths considered are $n = 30\text{k}, 40\text{k}, \ldots, 200\text{k}$. The simulation process was replicated 500 times for each estimator and chain size combination.

It's impractical to display the mixing properties for all 19 coefficients in brevity. Therefore, we concentrate on two coefficients for illustrative purposes, noting that the remaining coefficients demonstrate similar properties. Figures 6 and 7 illustrate strong correlation in the mixing properties for the intercept and loan duration coefficients. Moreover, density plots exhibit reasonable patterns, suggesting appropriate mixing within the chain.

The relationship between simulation size and and $\widehat{\text{ESS}}/n$ is illustrated on the left side of Figures 8-10 across the different estimation techniques. The median computation time are also presented on the right side of Figures 8-10. To ease comparison, Tables 2 and 3 provide numerical estimates and compute times for the terminal chain length of 200k.

Observe that Σ_n is in the denominator for the estimator $\widehat{\text{ESS}}$ in 5, thus if Σ_n is negatively biased $\widehat{\text{ESS}}$ can become inflated. We observe this behavior in the left hand side of Figures 8-
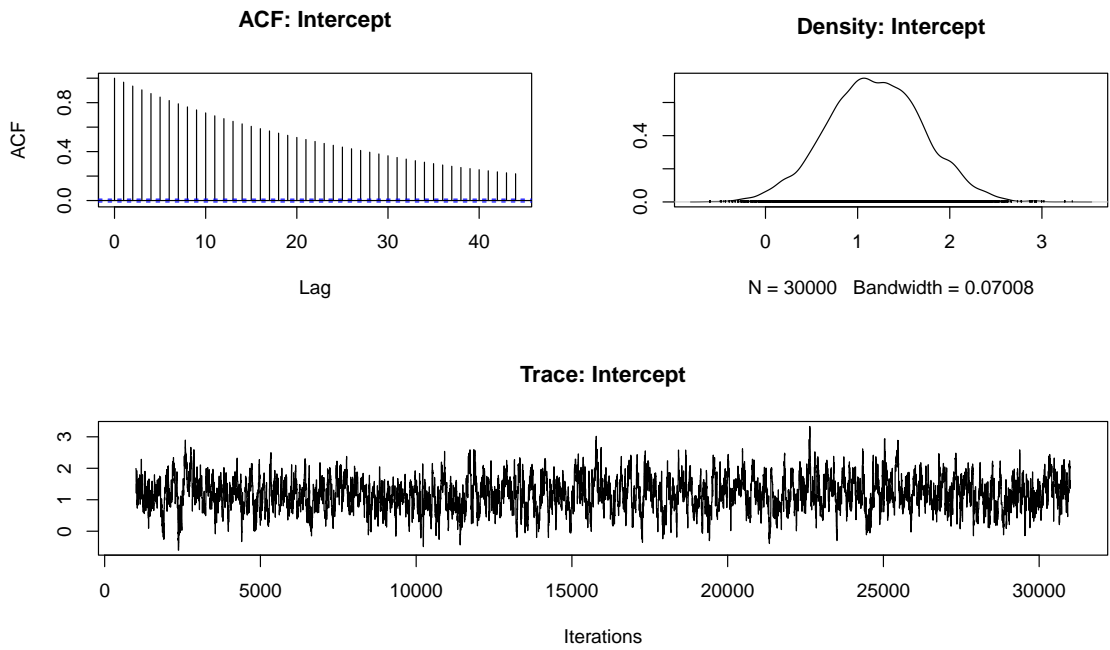
ACF: Intercept

Density: Intercept

Trace: Intercept

Figure 6: Mixing properties of the the intercept coefficient.

ACF: Duration Coef

Density: Duration Coef
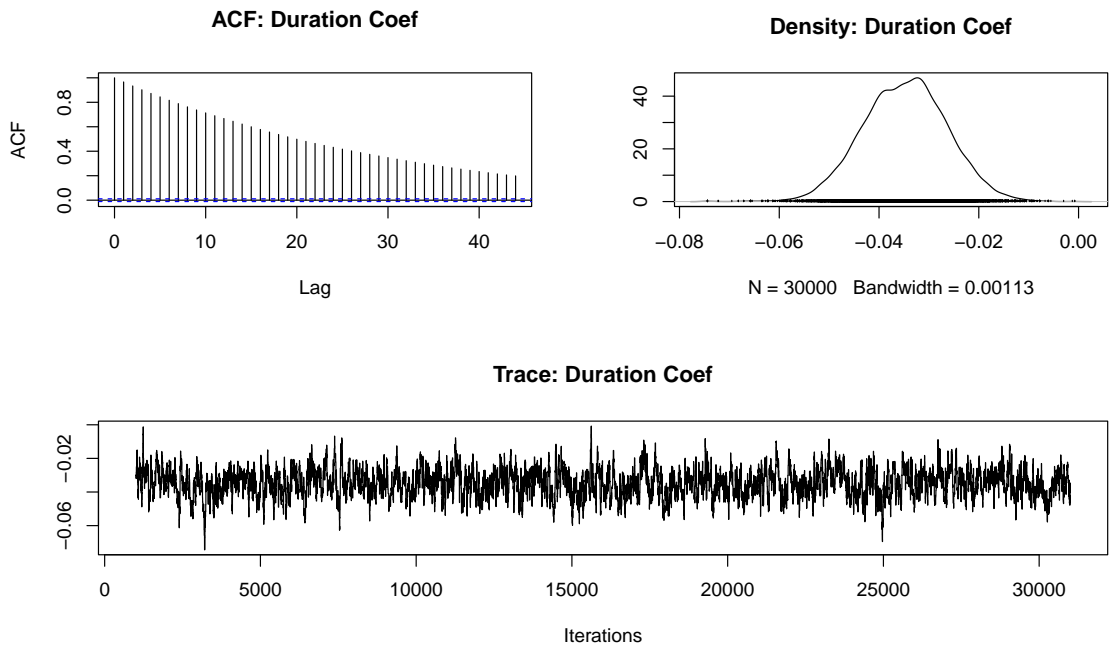
Trace: Duration Coef

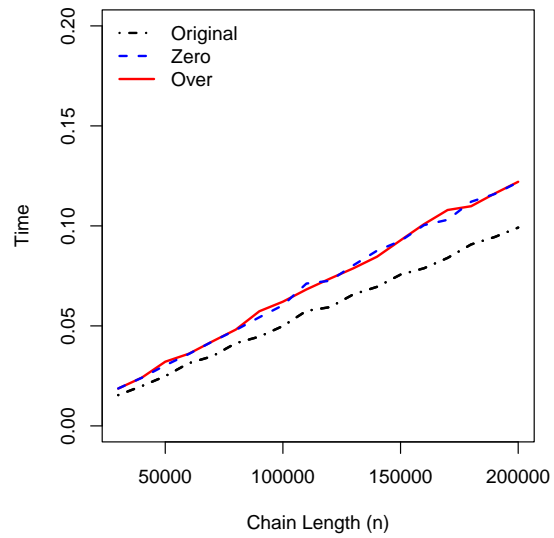Figure 7: Mixing properties of the loan duration coefficient.
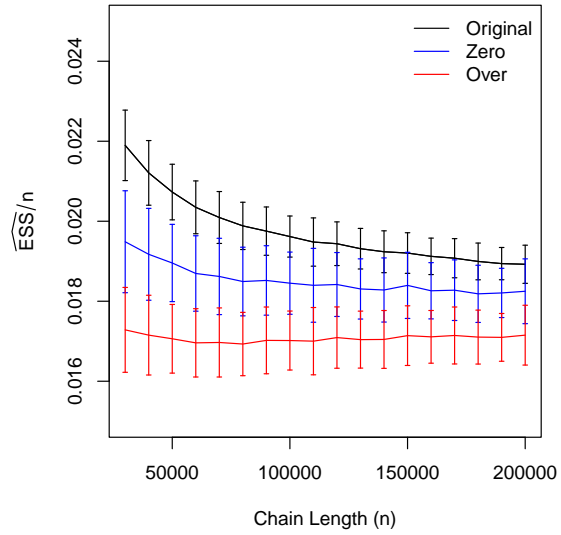
Figure 8: Plots of $\widehat{\mathrm{ESS}}/n$ and median computation time for the BM estimator.
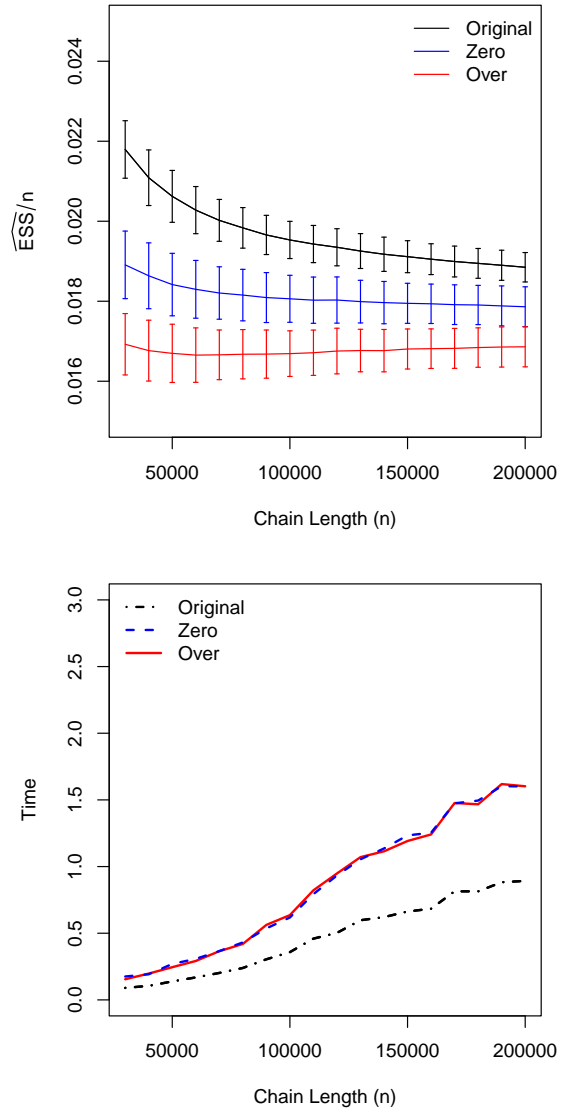
Figure 9: Plots of $\widehat{\text{ESS}}/n$ and median computation time for the SV estimator.

10 for the original SV and BM estimators, where $\widehat{\mathrm{ESS}}$ converges from above and eventually stabilizes. This convergence from above can result in premature chain termination when using the guidelines described in Section 2.

In contrast to the original estimators, the zero and over lugsail adjustments result in a less biased Σ_n. The consequences of this reduced bias is immediately observed via the faster rate of convergence for $\widehat{\mathrm{ESS}}$. The over lugsail setting has the added feature that it typically converges from below, a characteristic procured due to a positively biased Σ_n. Thus, the over lugsail may result in running a chain slightly longer than necessary yielding a more favorable conservative approach to termination. The initial sequence estimator also has an improved convergence rate in comparison to the original SV and BM estimators, but it does not converge as fast as the over lugsail and it does not seem to converge from above in this example.

We further observe the error bars which indirectly indicate estimation variability of Σ_n. As expected, the error bars are larger for the zero and over lugsail settings compared to the original estimator for both the SV and BM methods. In addition, the simulation illustrated a decrease in the variability of $\widehat{\mathrm{ESS}}$ as the chain increases for all settings. The difference of variability between the estimators is marginal, with the the initial sequence estimator is generally higher than the SV and BM methods.

	Original	Zero	Over
Batch Means	0.01892 (0.00029)	0.01825 (0.00049)	0.01715 (0.00045)
Spectral Variance	0.01885 (0.00022)	0.01786 (0.00030)	0.01686 (0.00030)
Initial Sequence	0.01758 (0.00050)		

Table 2: Average $\widehat{\mathrm{ESS}}/n$ with a chain length of $n = 200k$.

	Original	Zero	Over
Batch Means	0.09915 (0.00317)	0.12180 (0.00474)	0.12210 (0.00452)
Spectral Variance	0.8926 (0.09265)	1.60100 (0.14400)	1.60200 (0.13480)
Initial Sequence	16.40000 (3.617)		

Table 3: Average time in seconds to calculate Σ_n with a chain length of $n = 200k$

Finally, Table 3 provides computation time across the estimation procedures for the terminal chain length of 200k. BM methods clearly have a more favorable computation time and the initial sequence method had the slowest. For example, we notice in Table 3 the computation time for original BM and SV estimators roughly differed by a factor of about 10. Moreover, the computation time between the SV and initial sequence estimators
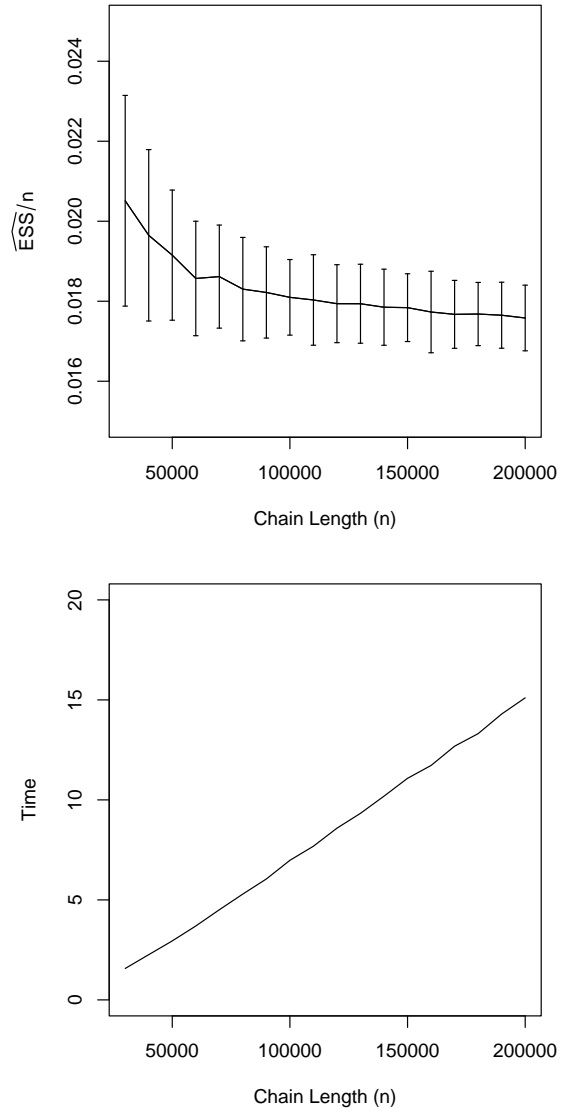
Figure 10: Plots of $\widehat{\mathrm{ESS}}/n$ and median computation time for the initial sequence estimator.

differed by over 15. Implementing the lugsail adjustments increased computation time for a given estimator, with relatively minimal discrepancy between the zero and over lugsail settings. For this setting the computation times across all settings is in terms of seconds, and the difference in computation times is largely inconsequential. However, with longer chain lengths and higher dimensions this difference will eventually become substantial.

7   Discussion

We explored various techniques for estimating Σ, the asymptotic covariance matrix from a Markov chain CLT. Our focus lies on scenarios commonly encountered in contemporary high-dimensional MCMC simulations. These scenarios involve concurrent estimation of multiple quantities, which are likely correlated, and where the Markov chain correlation tends to be positive and strong. Moreover, the simulations involve an extensive number of iterations. Within these constraints, we identify diverse methods for estimating Σ beyond the prevalent BM estimator.

For other scenarios with correlated data, variance estimators often follow a structure akin to Σ. For instance, in time series analysis Σ emerges in the context of spectral estimation and the determination of long-run variance (Hannan, 1970; Priestley, 1981). In econometrics, it is referred to as heteroskedastic and autocorrelation consistent covariance matrix estimation (Andrews, 1991; Newey and West, 1987). While the literature concerning the estimation of Σ in time-series and econometric applications is still expanding, these contexts typically revolve around moderate levels of correlation, a relatively limited number of available data points for estimation purposes, and smaller number of dimensions, see e.g. Lazarus et al. (2018).

It is essential to underscore that the estimation of the LRV in correlated data scenarios continues to be an active research area. Chan and Yau (2017) propose a recursive estimator using a sequence of batch sizes that increase with n, while Alexopoulos et al. (2007) considers overlapping batching methods for steady-state simulation output. Other general techniques include standardized time series weighted area estimators (Goldsman et al., 1990) and subsampling bootstrap variance estimators (Politis et al., 1999).

Specialized approaches include estimates of Σ based on regenerative simulations (Hobert et al., 2002), solutions of the Poisson equation (Douc et al., 2022), and shape-constrained estimators based on underlying restrictions similar to initial sequence estimation (Berg and Song, 2022). Additionally, McElroy and Politis (2024) address LRV estimation through local polynomial regression on the periodogram of spectral density function at zero. Estimation of the asymptotic covariance matrix in nonstationary time series has also been addressed

in the presence of change points (Chan, 2022a,b). Nonetheless, estimating Σ in truly high-dimensional problems remains challenging.

A practitioner may be tempted to select the widely used BM method without much consideration of the setting. However, all the discussed estimation methods are valid and should be considered. The choice of estimator revolves around underlying correlation, computational costs, and downstream analysis, particularly estimating the ESS and evaluating parameter MCSEs to create confidence intervals.

Lugsail transformations for both BM and SV estimators are more effective in the presence of high correlation, preventing premature termination with only a marginal increase in computational burden. However, over lugsails may over inflate the MCSE for the parameters of interest. Compared to the BM method, SV estimation increases computational burden but offers only a marginal improvement in MCSE and ESS estimation. The initial sequence estimator serves a similar purpose but involves a substantial increase in computational complexity and minimal tuning parameter adjustment.

Each method offers unique advantages, and a definitive choice is not always apparent. Therefore, the objective of Σ estimation is less about achieving optimality and more about making well-informed decisions.

Acknowledgments

References

Aktaran-Kalaycı, T., Alexopoulos, C., Argon, N. T., Goldsman, D., and Wilson, J. R. (2007). Exact expected values of variance estimators for simulation. *Naval Research Logistics (NRL)*, 54:397–410.

Alexopoulos, C., Argon, N. T., Goldsman, D., Tokol, G., and Wilson, J. R. (2007). Overlapping variance estimators for simulation. *Operations Research*, 55(6):1090–1103.

Anderson, T. W. (1994). *The Statistical Analysis of Time Series*. Wiley-Interscience.

Andrews, D. W. (1991). Heteroskedasticity and autocorrelation consistent covariance matrix estimation. *Econometrica*, 59:817–858.

Argon, N. T. and Andradóttir, S. (2006). Replicated batch means for steady-state simulations. *Naval Research Logistics (NRL)*, 53(6):508–524.

Berg, S. and Song, H. (2022). Efficient shape-constrained inference for the autocovariance sequence from a reversible Markov chain. *arXiv preprint arXiv:2207.12705*.

Brooks, S. P. and Gelman, A. (1998). General methods for monitoring convergence of iterative simulations. *Journal of Computational and Graphical Statistics*, 7:434–455.

Chakraborty, S., Bhattacharya, S. K., and Khare, K. (2022). Estimating accuracy of the MCMC variance estimator: Asymptotic normality for batch means estimators. *Statistics & Probability Letters*, 183:109337.

Chan, K. W. (2022a). Mean-structure and autocorrelation consistent covariance matrix estimation. *Journal of Business & Economic Statistics*, 40(1):201–215.

Chan, K. W. (2022b). Optimal difference-based variance estimators in time series: A general framework. *The Annals of Statistics*, 50(3):1376–1400.

Chan, K. W. and Yau, C. Y. (2017). Automatic optimal batch size selection for recursive estimators of time-average covariance matrix. *Journal of the American Statistical Association*, 112:1076–1089.

Chang, Y., Lu, Y., and Park, J. (2021). Understanding regressions with observations collected at high frequency over long span.

Chen, D.-F. R. and Seila, A. F. (1987). Multivariate inference in stationary simulation using batch means. In *Proceedings of the 19th Conference on Winter Simulation*, pages 302–304. ACM.

Dai, N. and Jones, G. (2017). Multivariate initial sequence estimators in Markov chain Monte Carlo. *Journal of Multivariate Analysis*, 159:325–342.

Damerdji, H. (1987). On strong consistency of the variance estimator. In *Proceedings of the 19th conference on Winter simulation*, pages 305–308. ACM.

Damerdji, H. (1991). Strong consistency and other properties of the spectral variance estimator. *Management Science*, 37:1424–1440.

Doss, C., Flegal, J. M., Jones, G. L., and Neath, R. C. (2014). Markov chain Monte Carlo estimation of quantiles. *Electronic Journal of Statistics*, 8:2448–2478.

Douc, R., Jacob, P. E., Lee, A., and Vats, D. (2022). Solving the Poisson equation using coupled Markov chains. *arXiv preprint arXiv:2206.05691*.

Flegal, J. M. and Gong, L. (2015). Relative fixed-width stopping rules for Markov chain Monte Carlo simulations. *Statistica Sinica*, 25:655–676.

Flegal, J. M., Haran, M., and Jones, G. L. (2008). Markov chain Monte Carlo: Can we trust the third significant figure? *Statistical Science*, 23:250–260.

Flegal, J. M., Hughes, J., Vats, D., Dai, N., Gupta, K., and Maji, U. (2021). *mcmcse: Monte Carlo Standard Errors for MCMC*. Riverside, CA, and Kanpur, India. R package version 1.5-0.

Flegal, J. M. and Jones, G. L. (2010). Batch means and spectral variance estimators in Markov chain Monte Carlo. *The Annals of Statistics*, 38:1034–1070.

Gelfand, A. E. and Smith, A. F. M. (1990). Sampling-based approaches to calculating marginal densities. *Journal of the American Statistical Association*, 85:398–409.

Gelman, A. and Rubin, D. B. (1992). Inference from iterative simulation using multiple sequences (with discussion). *Statistical Science*, 7:457–472.

Genz, A., Bretz, F., Miwa, T., Mi, X., Leisch, F., Scheipl, F., and Hothorn, T. (2018). mvtnorm: Multivariate Normal and *t* distributions. R package version 1.0-8.

Geyer, C. J. (1992). Practical Markov chain Monte Carlo. *Statistical science*, pages 473–483.

Geyer, C. J. (2011). Introduction to Markov chain Monte Carlo. In *Handbook of Markov Chain Monte Carlo*. CRC, London.

Goldsman, D., Meketon, M., and Schruben, L. (1990). Properties of standardized time series weighted area variance estimators. *Management Science*, 36(5):602–612.

Gong, L. and Flegal, J. M. (2016). A practical sequential stopping rule for high-dimensional Markov chain Monte Carlo. *Journal of Computational and Graphical Statistics*, 25:684–700.

Gupta, K. and Vats, D. (2020). Estimating Monte Carlo variance from multiple Markov chains. *arXiv preprint arXiv:2007.04229*.

Hannan, E. J. (1970). *Multiple Time Series*. Wiley (New York, NY).

Hobert, J. P., Jones, G. L., Presnell, B., and Rosenthal, J. S. (2002). On the applicability of regenerative simulation in Markov chain Monte Carlo. *Biometrika*, 89:731–743.

Hofmann, H. (1994). Statlog (German Credit Data). UCI Machine Learning Repository. DOI: https://doi.org/10.24432/C5NC77.

Jones, G. L. (2004). On the Markov chain central limit theorem. *Probability Surveys*, 1:299–320.

Jones, G. L., Haran, M., Caffo, B. S., and Neath, R. (2006). Fixed-width output analysis for Markov chain Monte Carlo. *Journal of the American Statistical Association*, 101:1537–1547.

Jones, G. L. and Hobert, J. P. (2001). Honest exploration of intractable probability distributions via Markov chain Monte Carlo. *Statistical Science*, 16:312–334.

Kass, R. E., Carlin, B. P., Gelman, A., and Neal, R. M. (1998). Markov chain Monte Carlo in practice: A roundtable discussion. *The American Statistician*, 52(2):93–100.

Kosorok, M. R. (2000). Monte Carlo error estimation for multivariate Markov chains. *Statistics and Probability Letters*, 46:85–93.

Lazarus, E., Lewis, D. J., and Stock, J. H. (2021). The size-power tradeoff in har inference. *Econometrica*, 89(5):2497–2516.

Lazarus, E., Lewis, D. J., Stock, J. H., and Watson, M. W. (2018). HAR inference: Recommendations for practice. *Journal of Business & Economic Statistics*, 36(4):541–559.

Liu, Y. and Flegal, J. M. (2018). Weighted batch means estimators in Markov chain Monte Carlo. *Electron. J. Statist.*, 12(2):3397–3442.

Liu, Y., Vats, D., and Flegal, J. M. (2021). Batch size selection for variance estimators in MCMC. *Methodology and Computing in Applied Probability*, pages 1–29.

McElroy, T. and Politis, D. N. (2024). Estimating the spectral density at frequencies near zero. *Journal of the American Statistical Association*, 119(545):612–624.

Meketon, M. S. and Schmeiser, B. (1984). Overlapping batch means: Something for nothing? In *WSC '84: Proceedings of the 16th conference on Winter simulation*, pages 226–230, Piscataway, NJ, USA. IEEE Press.

Meyn, S. and Tweedie, R. (2009). *Markov Chains and Stochastic Stability*, volume 2. Cambridge University Press Cambridge.

Newey, W. K. and West, K. D. (1987). A simple, positive semi-definite, heteroskedasticity and autocorrelation consistent covariance matrix. *Econometrica*, 55:703–708.

Parzen, E. (1957). On consistent estimates of the spectrum of a stationary time series. *The Annals of Mathematical Statistics*, pages 329–348.

Politis, D. N. and Romano, J. P. (1995). Bias-corrected nonparametric spectral estimation. *Journal of Time Series Analysis*, 16(1):67–103.

Politis, D. N. and Romano, J. P. (1996). On flat-top kernel spectral density estimators for homogeneous random fields. *Journal of Statistical Planning and Inference*, 51(1):41–53.

Politis, D. N., Romano, J. P., and Wolf, M. (1999). *Subsampling*. Springer-Verlag Inc.

Priestley, M. B. (1981). *Spectral analysis and time series*. Academic press, London.

Robert, C. P. and Casella, G. (2004). *Monte Carlo Statistical Methods*. Springer, New York, second edition.

Robertson, N., Flegal, J. M., Vats, D., and Jones, G. L. (2021). Assessing and visualizing simultaneous simulation error. *Journal of Computational and Graphical Statistics*, 30(2):324–334.

Sun, Y. (2013). A heteroskedasticity and autocorrelation robust F test using an orthonormal series variance estimator. *The Econometrics Journal*, 16(1):1–26.

Sun, Y. (2014). Let's fix it: Fixed-b asymptotics versus small-b asymptotics in heteroskedasticity and autocorrelation robust inference. *Journal of Econometrics*, 178:659–677.

Sun, Y. and Phillips, P. C. (2008). Optimal bandwidth choice for interval estimation in GMM regression. *Working Paper*.

Vats, D. and Flegal, J. M. (2022). Lugsail lag windows for estimating time-average covariance matrices. *Biometrika*, 109(3):735–750.

Vats, D., Flegal, J. M., and Jones, G. L. (2018). Strong consistency of multivariate spectral variance estimators in Markov chain Monte Carlo. *Bernoulli*, 24:1860–1909.

Vats, D., Flegal, J. M., and Jones, G. L. (2019). Multivariate output analysis for Markov chain Monte Carlo. *Biometrika*, 106:321–337.

Vats, D. and Knudson, C. (2021). Revisiting the Gelman-Rubin Diagnostic. *Statistical Science*, 36(4):518 – 529.

Vats, D., Robertson, N., Flegal, J. M., and Jones, G. L. (2020). Analyzing markov chain monte carlo output. *WIREs Computational Statistics*, 12(4):e1501.

Welch, P. D. (1987). On the relationship between batch means, overlapping means and spectral estimation. In *WSC '87: Proceedings of the 19th conference on Winter simulation*, pages 320–323, New York, NY, USA. ACM.